IAC-06-C1.8.06

NEXT GENERATION GNSS FOR NAVIGATION OF FUTURE SAR CONSTELLATIONS

Werner Enderle
Queensland University of Technology, Australia
w.enderle@qut.edu.au

Hauke Fiedler, Sergio De Florio, Gerhard Krieger, Friedrich Jochim
German Aerospace Center (DLR), Microwaves and Radar Institute, Germany
Hauke.Fiedler@dlr.de, SergioDeFlorio@dlr.de , Gerhard.Krieger@dlr.de, Fritz.Jochim@dlr.de,

Simone D'Amico
German Aerospace Center (DLR), German Space Operations Center, Germany
Simone.DAmico@dlr.de,

Shannon Dawson, William Kellar
Queensland University of Technology, Australia
s.dawson@qut.edu.au, w.kellar@qut.edu.au

ABSTRACT

The next Generation of Global Satellite Navigation Systems (GNSS - GPS and Galileo) will provide enhanced performance with respect to signals, services, quality and quantity of measurements, availability, integrity and accuracy. Since in 2004, the European Commission (EC) and the USA signed an agreement about the compatibility and interoperability between GPS and Galileo, the combined use of both systems and respective measurements will have a significant impact on the design of future navigation systems in general.

This paper will present results from simulations for a SAR formation flying mission. Applicability, advantages and limitations of GNSS based concepts for orbit- and attitude determination in the context of SAR formation missions in LEO will be outlined and discussed.

INTRODUCTION

The upcoming potential for the development of new navigation systems is very important in the context of future, more challenging and complex requirements for space missions, especially into the Low Earth Orbit (LEO). One of the key elements for future missions is the maximization of onboard autonomy. This is especially true for the realization of new Synthetic Aperture Radars (SAR) mission

concepts, based on formation flying in close formation (less than 30m distance) in LEO and dedicated to SAR interferometry missions. Such concepts may be based on onboard navigation concepts for real time orbit and attitude control. The requirements for onboard orbit determination depend on the requested SAR interferometric baseline and thus on the SAR frequency band used. For future SAR missions a post processed relative position accuracy of less than 1mm in case of X-band observations will be required.

For SAR interferometry, many formations were proposed like e.g. TechSAT, Cartwheel, or Pendulum [1,2]. Such missions, suitable for X-band, C-band or L-band applications [3,4,6,7,8], were investigated based on state-of-the-art onboard navigation capabilities. The envisaged GNSS possibilities open a new challenge for SAR interferometric observations with respect to lower orbits, higher efficiency as well as improved use of X-band SAR. As in the previous papers a constellation of one active master satellite (e.g. TerraSAR-X, ENVISAT, RADARSAT, ALOS, etc.) and three small slave satellites will be proposed. The slave satellites are assumed to be passive in the sense that their SARs receive only the SAR signal reflected from the pixel illuminated by the master satellite.

SAR FORMATION

For this study the most challenging orbital height of about 500 km will be selected. The master satellite is assumed to move on a sunsynchronous orbit with frozen eccentricity. A formation of three slave satellites will be kept within a distance of 20-50km from the master. The reference point of the slave satellites will move on the same orbit as the master satellite in front of or following the master.

The slave satellites within their formation have the following arrangement: satellite 2 is the reference satellite of the formation, moving on a sun synchronous orbit like the master satellite with frozen eccentricity. Satellite 1 will move on a HELIX [11] with a separation of 300 m at equator crossing and 30 m at the northern/southern turn. Satellite 3 will similarly move on a HELIX but with a separation of 30 m at equator crossing and 30 m at the northern/southern turn (cf. Fig. 1).

The motion of satellite 3 relative to satellite 2 for one draconic period is visualized in Fig. 1. Due to the projections on the basic planes of the co-moving coordinate system, the safety of the orbits with respect to collision risk can easily be analysed.

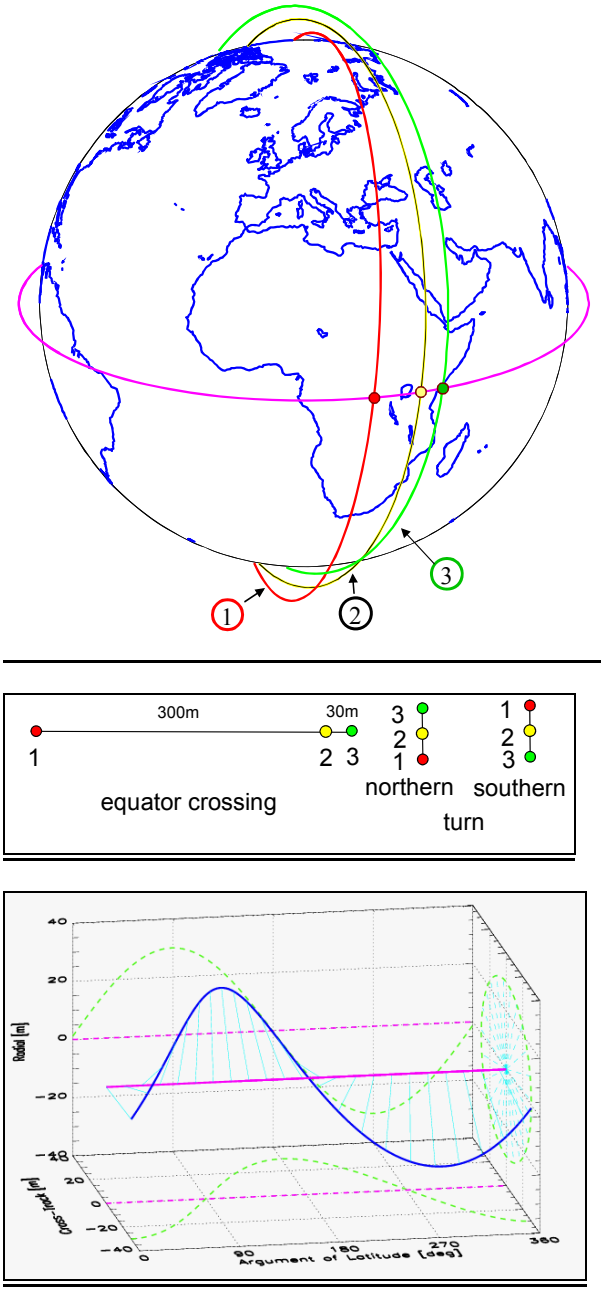

Fig 1: Relative motion of satellite 3 with respect to satellite 2 vs. argument of latitude for one draconic period. The relative orbit of satellite 2 is plotted in magenta, the relative orbit of satellite 3 in dark blue. Their respective projections onto the radial/cross-track/along track planes are coloured green. The baseline vector between satellite 2 and satellite 3 is plotted in cyan.

Table 1 summarizes the mean Keplerian elements of all four satellites. The values for right ascension of the ascending node and for the mean anomaly are relative figures.

Parameter	Master	Satellite 1	Satellite 2	Satellite 3
Orbit height [km]	500	500	500	500
Eccentricity	0.0	0.00000436	0.0	0.00000436
Long periodic Eccentricity	0.00117349	0.00117785	0.00117349	0.00117785
Inclination	97°.4247	97°.4247	97°.4247	97°.4247
RAAN	0	359°.997310	0°.0	0°.000269
Argument of Perig.	90°	90°	90°	270°
Mean Anomaly	270°+x	270°	270°	90°

Table 1: Absolute Mean Keplerian orbital parameters for master and slave satellites

Table 2 summarize the relative orbital elements of the three slave satellites with respect to each other. In particular the magnitude/phase of the relative eccentricity and inclination vectors are provided together with the relative semi major axis and mean argument of latitude.

Parameter	s/c-1 w.r.t. s/c-2	s/c-3 w.r.t s/c-2	s/c-3 w.r.t s/c-1
Eccentricity separation **a δe [m]**	30	30	60
Relative argument of perigee **φ [°]**	180°.0	0°.0	180°.0
Nodal separation **δΩ [m]**	300	30	330
Relative argument of latitude **θ [°]**	0°.0	0°.0	0°.0
Relative semimajor axis **Δa [m]**	0	0	0
Relative mean argument of latitude **aΔu [m]**	0	0	0

Table 2: Relative orbital parameters of satellites 1 and 3 with respect to satellite 2 and of satellite 3 with respect to satellite 1

The relative orbital elements description shows that the eccentricity/inclination vector separation concept [10] is correctly applied to all s/c couples. The risk of collision is minimized for the formation even in presence of large along-track uncertainties and contingencies. The formation is operationally safe due to the parallel orientation of the relative eccentricity and inclination vectors.

The slave satellites are assumed to be micro-satellites. They are passive with respect to SAR observation. An AOCS must be implemented in order to allow relative and absolute orbit correction maneuvers as well as attitude 3-axis stabilization for antenna steering and inter-satellite link (ISL) communication. The satellite data for the slaves are summarized in Table 3. The relative orbit control accuracy is justified from a SAR point of view.

Parameter	Micro-satellites
Satellite mass	200 kg
Cross section area	2 m^2
Mission time	2 years
Distance of master to formation	20 – 50 km

Table 3: Parameters for the micro-satellites.

Orbit -and Attitude Determination (OD and AD) accuracy requirements for the proposed SAR formation, which are relevant to this research, are shown in Table 4.

Orbit -and Attitude Requirements	Values	On-Board
Relative orbit control accuracy of micro-satellite	± 3 m (3D, 1σ)	yes
Relative baseline vector 3D for X-band	< 1 mm (3D, 1σ)	**no**
Attitude accuracy for each axis	[0.01°;0.07°] (3 σ)	yes

Table 4: Orbit and Attitude Accuracy Requirements. Note the relative baseline vector accuracy is for post processing not for on board

GNSS APPLICATIONS FOR SATELLITE CONSTELLATIONS

GNSS – GPS and Galileo

GPS is a well established system and applications for space are constantly growing. Galileo, the European Global Navigation Satellite System is currently under development and the first test satellite GIOVE-A has been successfully launched in December 2005. Detailed information about Galileo is given in [12]. Information about GPS are widely distributed, see e.g. [13]. One of the main differences between the US American GPS and Galileo is that GPS is military operated, whereas Galileo is designed as a civil operated system under European control and commercially oriented. Extensive research has been done in the area of Galileo signal design (e.g. see [15]). The Galileo signals are different compared to existing GPS signals in from of; Code

structure, larger signal bandwidth, increased power, more frequencies and combinations of code with no data modulated on and frequencies with high data rates. The sum of all these features resulting in a superior performance compared to the existing GPS. However, the signal design in Galileo is an ongoing coordination and optimization process and not finished yet. One of the key features of future GNSS (GPS + Galileo) will be the agreed compatible and interoperable for the civil signals between Galileo and GPS. A consequence of this agreement between the USA and the European Commission is the option for a joint use of both systems for civil signals on signal level. Galileo will provide a total of five services, including four navigation services on four frequencies and 10 signals. Fig. 2 shows the Galileo Signal and Frequency baseline plan. By mapping the Galileo signals to services, it becomes clear that a wide variety of options regarding the choice of GNSS receiver configurations exists. The services and signals from GNSS, which have been used within this simulations are given in Table 5. The chosen services are the signals on the Galileo Open Service and GPS civil service on L1 and L5. Both services will be available free of charge. It should be clearly mentioned that the chosen Galileo signal/service combination is not the ultimate services related to expected accuracy. However, the potentially more accurate services are subject to fees and have not been investigated in the context of this research, but will be in the context of other research.

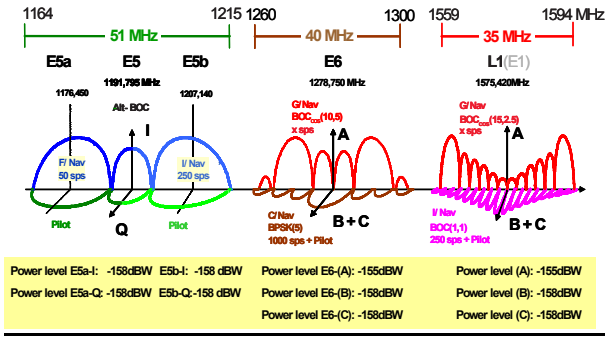

Fig 2: Galileo Signal and Frequency Plan – Baseline

System	Service	Num Frequencies	Frequencies used
Galileo	Open Service (OS)	3	L1 and E5a, (E5b)
GPS	C/A	2	L1 and L5

Table 5: GNSS Signals and Frequencies used for Simulations within this study

Simulations

The main objective of this research was to investigate in which way the future available GNSS signals and services can be used for on-board navigation in the context of a SAR satellite formation (SAR Orbit parameters outlined in Table 1 and Table 2) and meet the accuracy requirements regarding OD and AD. The simulations conducted within this research are summarized in Table xxx.

Simulation	Model	Tool
SAR Constellation	• Precise Orbit Propagator Gravity Model JGM3 (70x70) • Third body gravitation effects • Earth Atmosphere	• GNSS ConstellationTool • ORBProp
GPS and Galileo Constellations	• Satellite constellations based on Kepler orbits •	• GNSS ConstellationTool
GNSS Measurements	• Code and Carrier Phase measurements calculated based on models and assumptions about error budgets for GPS and Galileo	• GNSS ConstellationTool • Satellite Navigation Toolbox 3.0

Table 6: Simulation Environment , used Models and Tools

ORBIT AND ATTITUDE DETERMINATION BASED ON SIMULATED GNSS DATA

GNSS Observations for Space Applications

GNSS users, including space applications, have basically the following GNSS measurements available; the Code Phase Pseudo Range measurement PR [m], the Carrier Phase Pseudo Range measurement Φ [m] and the Doppler measurement D [m/s] for each individual frequency. Equations (1) to (3) outlining the models for the above mentioned measurements.

$$PR^{s}_{r,j}(t) = \rho^{s}_{r}(t) + c(dT_{r,j} - dt^{s,i}) + d^{s}_{r,j_{ion}}(t) + \varepsilon^{s}_{r,j_{mp}}(t) + \varepsilon_{r,j_{Rx}}(t) \quad (1)$$

$$\Phi^{s}_{r,j}(t) = \rho^{s}_{r}(t) + c(dT_{r,j} - dt^{s,i}) - d^{s}_{r,j_{ion}}(t) + \varepsilon^{s}_{r,j_{mp}}(t) + \varepsilon_{r,j_{Rx}}(t) - \lambda_j N^{s}_{r,j} \quad (2)$$

$$D^{s}_{r,i}(t) = \dot{\rho}^{s}_{r}(t) + c\left(\dot{\delta}_{tmr}(t) - \dot{\delta}^{s}_{tsv}(t)\right) \quad (3)$$

The terms, used within equation (1), (2) and (3) are; ρ is the slant range, c the velocity of light in vacuum, dT is the clock error in the GNSS receiver, dt is the clock error in the GNSS satellite, d_{ion} is the Ionospheric error, ε_{mp} is the multi path error, ε_{Rx} is the residual error resulting from user equipment, λ is the wavelength of the individual signal and N is the Cycle Ambiguity on a specific frequency. Further, the indices are j, for frequency, s for satellite and r for receiver.

Base on the availability of multiple frequencies, adequately separated from each other, one can generate an Ionospheric free observation for code and carrier phase measurements. The Ionospheric free code observation was used within this research as the fundamental observation for the on-board OD process. The Ionospheric free observation e.g Galileo frequency combination L1 and E5a can be written in the following form:

$$PR^{s}_{IF,r,L1}(t) = \frac{f^2_{L1}}{f^2_{L1} - f^2_{E5a}} PR^{s}_{r,L1}(t) - \frac{f^2_{E5a}}{f^2_{L1} - f^2_{E5a}} PR^{s}_{r,E5a}(t) \quad (4)$$

An equivalent equation can be obtained for GPS observations.

Orbit Determination Concept

The accuracy requirements, as outlined in Table 4 are the drivers for the investigated on-board Orbit Determination (OD) concept. The proposed concept is a Batch Least Square Method (LSQ) using Ionospheric free Code Pseudo Range observations from Galileo, GPS or from both systems.

Orbit Dynamic Model

The orbit dynamic model, used for the Orbit Prediction (OP) plays a key role for the applicable data arc length used in the LSQ. By comparison (see Fig. 3) between a highly accurate orbit model with the implemented JGM3 gravity model with order and degree of 10, it can be seen that the JGM3 (10x10) gravity model produces a 3D position error of about 3 m within a period of 10 min and a 3D position error of about 1 m in 5 min. A data arc length of 5 min has been chosen for the OD process. This provides a margin with respect to the 3D position accuracy requirement (3 m, 1σ) of about 2 m. Subsequently the OD process has to provide an position accuracy better than 2 m for a 5 min data arc. A sampling rate of 1Hz was used within this simulation. The dynamic equation of motion for the satellite reference orbit generation can be expressed as:

$$\ddot{\mathbf{r}}_I = \nabla U_{(10x10)} \quad (5)$$

where U is the Earth gravity potential and $\ddot{\mathbf{r}}_I$ is the satellite acceleration expressed in the inertial coordinate system (J2000). The calculations of the spherical harmonic terms, needed for the numerical integration of the dynamical equations of motion are conducted according to Cunningham. The numerical integration of equation (5) was done by applying a 4th order Runge-Kutta method.

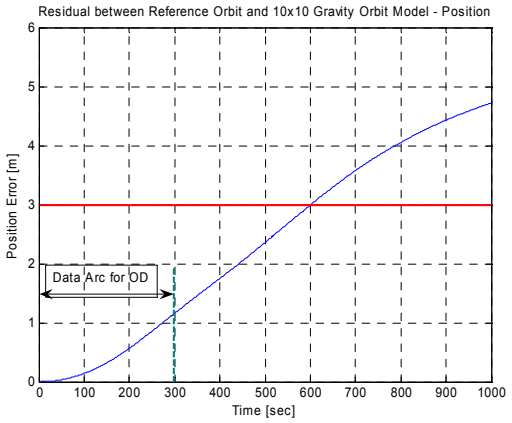

Fig. 3: Selected Data Arc interval of 5 min for Orbit Determination process

Observation Model for OD

The Galileo and GPS observation model – Ionospheric free Pseudo Range measurements for a single epoch t is outlined in equation (4). No carrier phase smoothing has been applied, which would have the noise level for the code observations further reduced The observation vector PR_{IF} can be formed in the following way:

$$\mathbf{PR}_{\mathrm{IF}} = \begin{bmatrix} \mathrm{PR}^{s,1}_{r,L1\_E5a,IF_{Gal}}(t) \\ \vdots \\ \mathrm{PR}^{s,n}_{r,L1\_E5a,IF_{Gal}}(t) \\ \mathrm{PR}^{s,1}_{r,L1\_L5,IF_{GPS}}(t) \\ \vdots \\ \mathrm{PR}^{s,m}_{r,L1\_L5,IF_{GPS}}(t) \end{bmatrix} \quad (6)$$

The state vector for the on-board OD is defined as:

$$\mathbf{x}_{\mathrm{I}} = [\mathbf{r}_{\mathrm{I}}, \mathbf{v}_{\mathrm{I}}]^{\mathrm{T}} = [\mathrm{r}_{\mathrm{x}}, \mathrm{r}_{\mathrm{y}}, \mathrm{r}_{\mathrm{z}}, \mathrm{v}_{\mathrm{x}}, \mathrm{v}_{\mathrm{y}}, \mathrm{v}_{\mathrm{z}}]^{\mathrm{T}}. \quad (7)$$

Orbit Determination Process – Batch Least Squares

The OD problem can be stated as the estimating of the state vector, $\mathbf{x}_{\mathrm{I}} = [\mathbf{r}_{\mathrm{I}}, \mathbf{v}_{\mathrm{I}}]^{\mathbf{T}}$, expressed in the inertial coordinate system for a specific epoch based on an adequate set of measurements by applying a Batch Least Squares method. The solution of this LSQ problem is well known and documented in the literature [ref].

$$\Delta\mathbf{x} = \left[\mathbf{H}^{\mathrm{T}}\mathbf{W}\mathbf{H}\right]^{-1} \cdot \mathbf{H}^{\mathrm{T}}\mathbf{W}\mathbf{l}. \quad (8)$$

The term $\mathbf{H}^{\mathrm{T}}\mathbf{W}\mathbf{H}$ and $\mathbf{H}^{\mathrm{T}}\mathbf{W}\mathbf{l}$ represents the sum over all epochs of the data arc. The weight matrix W is a diagonal matrix and provides a weighting for all measurements obtained from GPS and Galileo. The elements of the weighting matrix are the 1σ values for the measurement errors of the Ionospheric free code Pseudo Range. Typical values within this research are for GPS around 2.5 m to 3.5 m, and for Galileo 0.6 m to 1.1 m. These values were depending on the assumed multipath environment conditions.

The residual vector $\mathbf{l}$ is the difference between the calculated measurements (based on predicted orbit) and the measurements itself. This vector can be calculated for each epoch according to:

$$\mathbf{l} = \mathbf{PR}_{\mathrm{IF\,obs}} - \mathbf{PR}_{\mathrm{IF\,calc}}. \quad (9)$$

The design matrix $\mathbf{H}$ is created from the observation matrix $\frac{\partial \mathbf{PR}_{\mathrm{IF}}}{\partial \mathbf{x}}$ and the state transition matrix $\phi(t, t_0)$. The functional relationship for the design matrix $\mathbf{H}$ is given by:

$$\mathbf{H} = \frac{\partial \mathbf{PR}_{\mathrm{IF}}}{\partial \mathbf{x}} \cdot \frac{\partial \mathbf{x}}{\partial \mathbf{x_0}} \quad (10)$$

The observation matrix for each epoch can be expressed as:

$$\frac{\mathbf{PR}_{\mathbf{IF}}}{\partial \mathbf{x}} = \left[\frac{\mathbf{PR}_{\mathbf{IF}}}{\partial \mathbf{r}_{\mathbf{I}}}, \frac{\mathbf{PR}_{\mathbf{IF}}}{\partial \mathbf{v}_{\mathbf{I}}}\right]. \quad (11)$$

The state transition matrix $\phi(t, t_0)$ is hereby defined as:

$$\phi(t,t_0) = \frac{\partial \mathbf{x}}{\partial \mathbf{x_0}}(t_i) = \begin{bmatrix} \frac{\partial \mathbf{r}}{\partial \mathbf{r_0}} & \frac{\partial \mathbf{r}}{\partial \mathbf{v_0}} \\ \frac{\partial \mathbf{v}}{\partial \mathbf{r_0}} & \frac{\partial \mathbf{v}}{\partial \mathbf{v_0}} \end{bmatrix}, \quad (12)$$

and the state transition's differential equation is given by:

$$\dot{\phi}(t,t_0) = \frac{\mathrm{d}}{\mathrm{dt}}\left[\frac{\partial \mathbf{x}}{\partial \mathbf{x_0}}\right]. \quad (13)$$

Equation 12 relates the state vector to the accelerations represented by the orbit dynamic model used for the calculation of the state transition matrix. In this work the state transmission matrix was calculated based on an approach proposed by Markley [ref]. Only the flattening of the Earth, J_2 was considered in the dynamic model for the state transition matrix. Detailed information about this approach can be found in [chira] and [enderle]. The final solution of the OD process can be obtained in an iterative way from:

$$\mathbf{x} = \mathbf{x_0} + \Delta\mathbf{x}. \quad (14)$$

The vector $\mathbf{x_0}$ is hereby an initial estimation of the state vector. This value can directly be obtained from the GNSS receiver position and velocity solution.

GNSS based Attitude Determination

The fundamental physical principle of the GPS based attitude determination process is the interferometric principle, which is shown in Fig. 4. The GPS receiver measures the carrier phase. From the carrier phase measurements, single difference (SD) carrier phase observations between two antennas and a GNSS satellite can be generated. For the simulations, it was assumed that the slave satellites will have four antennas, arranged in a rectangular configuration as outlined in Fig. 4

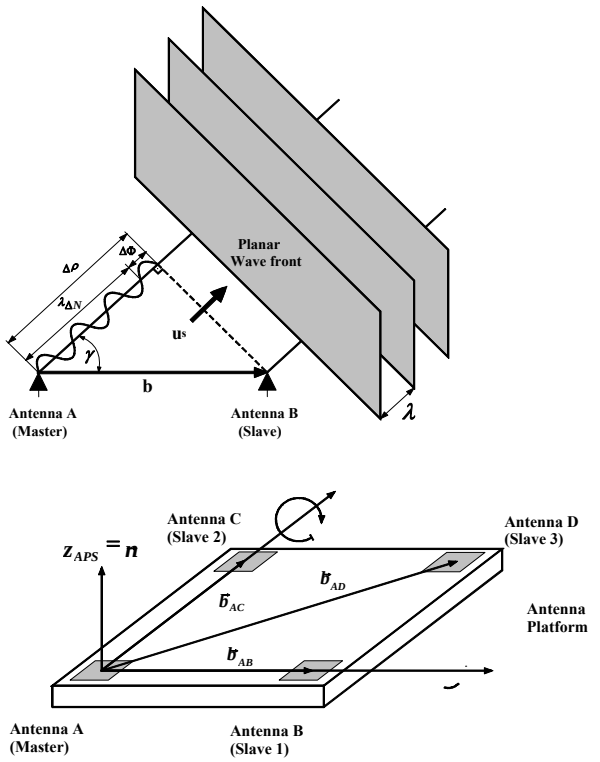

Fig. 4: Interferometric Principle and Attitude Sensor Array

The basic equations for the AD algorithm using SD and Euler Angles (Euler rotation sequence 3-1-2) as attitude parameters are outlined below.

$$\Delta\Phi^{i}_{m} = \Delta\rho^{i}_{m} - \lambda\Delta N^{i}_{m} \quad (15)$$

$$\Delta\rho^{i}_{m} = \mathbf{u}^{i}_{smB} \cdot \mathbf{b}_{mB} \quad (16)$$

$$\mathbf{u}^{i}_{smB} = \mathbf{A}\left(\phi,\theta,\psi\right) \cdot \mathbf{u}^{i}_{smR} \quad (17)$$

Equation (15) is the observation equation for the ideal case, neglecting any error. Equation (16) describes the SD slant range as a function of the Line Of Sight (LOS) unit vector and the corresponding baseline vectors, and equation (17) describes the relationship between the LOS vectors in the body fixed coordinate system B and the reference system R. Substitution of equations (15) and (17) into equation (16) and also considering an error term, leads to the general observation equation (18) for SD carrier phase measurements as a function of the Euler angles. The resulting SD observation equation for a frequency is given by:

$$\Delta\Phi^{i}_{m} = \left[\mathbf{A}\left(\phi,\theta,\psi\right) \cdot \mathbf{u}^{i}_{smR}\right] \cdot \mathbf{b}_{mB} - \lambda\Delta N^{i}_{m} + \Delta\varepsilon \quad (18)$$

where $\Delta\Phi$ is the SD carrier phase, $_m$ is the index for the baseline and $_i$ is the index for the GNSS satellites, which has been used for the generation of the SD. **A** represents the attitude matrix. The vector **u** is the LOS unit vector expressed in the reference co-ordinate system R, **b** is the baseline vector expressed in the body fixed co-ordinate system, λ is the wave length of the GNSS signal, ΔN is the difference of the initial number of cycle ambiguities and the term $\Delta\varepsilon$ represents errors, such as line bias, receiver noise and multipath effects.

The carrier phase cycle ambiguity ΔN can be solved in real time by MCAR techniques (see ref []). The state vector **x,** is represented by:

$$\mathbf{x} = \left[\phi,\theta,\psi\right]^{T}. \quad (19)$$

The minimum required number of visible GNSS satellites for the User is two in order to be able to perform a deterministic attitude solution. In case that the number of visible GPS satellites is > 2, a Least Square Solution (LSQ) will be used in a sequential way. The AD solution will be obtained by:

$$\Delta\mathbf{x} = \left[\mathbf{M}^{T} \cdot \mathbf{M}\right]^{-1} \cdot \mathbf{M}^{T} \cdot \mathbf{l} \quad (20)$$

with $\Delta\mathbf{x} = \left[\Delta\phi,\Delta\theta,\Delta\psi\right]^{T}$ is the solution vector. The vector l contains the residuals between calculated and measured observation, and the design matrix **M** is given by:

$$\mathbf{M} = \frac{\partial(\Delta\Phi)}{\partial \mathbf{x}} \qquad (21)$$

where x_0 is an initial state vector. The AD solution in the sense of the LSQ is given by:

$$\mathbf{x} = \mathbf{x}_0 + \Delta\mathbf{x}\,. \qquad (22)$$

The accuracy of GNSS based AD is depending on the geometry, the baseline length and the measurement errors. The most significant measurement error on the carrier phase is resulting from multipath. However, this is strongly depending on the design of the spacecraft and possible points and surfaces for reflection of signals. A multipath error of 2.5mm (1σ, SD) was assumed for the simulations. This reflects a low multi path environment. It was also assumed that the multipath error has a Gaussian distribution. The baseline length was considered 1 m between the master antenna and the slave antenna A and B. The resulting 1σ attitude accuracy can be calculated in the following way:

$$\begin{aligned}
\sigma_{\text{Att}} &= \frac{\sigma_{\text{SD}}}{b}\,\text{ATTDOP} \\
\sigma_{\text{Yaw}} &= \frac{\sigma_{\text{SD}}}{b}\,\text{YawDOP} \\
\sigma_{\text{Roll}} &= \frac{\sigma_{\text{SD}}}{b}\,\text{RollDOP} \qquad (23) \\
\sigma_{\text{Pitch}} &= \frac{\sigma_{\text{SD}}}{b}\,\text{PitchDOP}
\end{aligned}$$

$$\text{ATTDOP} = \sqrt{\text{RollDOP}^2 + \text{PitchDOP}^2 + \text{YawDOP}^2}$$

The DOP values are obtained from the covariance matrix $\text{Cov} = \left[\mathbf{M}^{\text{T}} \cdot \mathbf{M}\right]^{-1}$ of the attitude LSQ solution.

RESULTS

Visibility

The antenna platform is assumed to be integrated in such a way on the satellite that the normal vector of the antenna array is pointing in a zenith direction, away from the Earth. In Figure 5, the visibility of GPS, Galileo and the combined constellation for an user is shown over a period of two hours, based on link budget calculations.

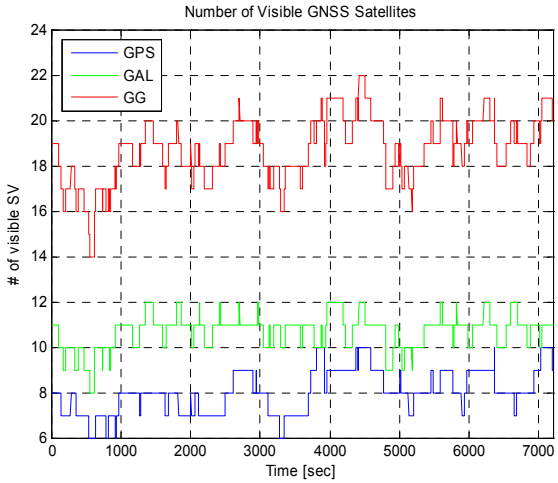

Fig. 5: Visibility of GNSS satellites for a space user with a zenith directed antenna array.

As it can be seen in Fig. 5, the use of GPS + Galileo will lead to a considerable increase of visible GNSS satellites, which is directly related to the amount of available observations for Orbit -and Attitude Determination and relative geometry between the constellations and the user in space.

Orbit Determination

The results obtained from the proposed OD concept by using Ionospheric free Code Pseudo Ranges observation within a LSQ process by using a data arc of 5 min. are shown in Table 7 and Table 8 and also illustrated in Fig. 6.

Solution Type	Values	OD Solution Error	1σ OD Accuracy	3D 1σ Pos Error [m]
GPS	Pos x [m]	1.671	0.528	**2.909**
	Pos y [m]	-1.742	0.666	
	Pos z [m]	-1.623	0.705	
	Vel x [m/s]	0.100514	0.002669	
	Vel y [m/s]	0.003025	0.003135	
	Vel z [m/s]	0.027869	0.003384	
Galileo	Pos x [m]	-0.080	0.466	**0.715**
	Pos y [m]	0.688	0.534	
	Pos z [m]	0.178	0.589	
	Vel x [m/s]	0.112068	0.002594	
	Vel y [m/s]	-0.006023	0.002547	
	Vel z [m/s]	0.020466	0.002846	
GPS + Galileo	Pos x [m]	0.076	0.416	**0.485**
	Pos y [m]	0.479	0.481	
	Pos z [m]	0.027	0.528	
	Vel x [m/s]	0.110785	0.002285	
	Vel y [m/s]	-0.005129	0.002290	
	Vel z [m/s]	0.020982	0.002550	

Table 7: Relative orbital parameters of satellites 1 and 3 with respect

The case shown in Table 7 is used in order to outline the impact of multipath on the

individual signals and its related impact on the overall OD performance. Fig. 6 shows a sample of 10 simulations in various environmental conditions. It can be clearly seen that the performance of Galileo based observations is significantly better than the performance of GPS based observations.

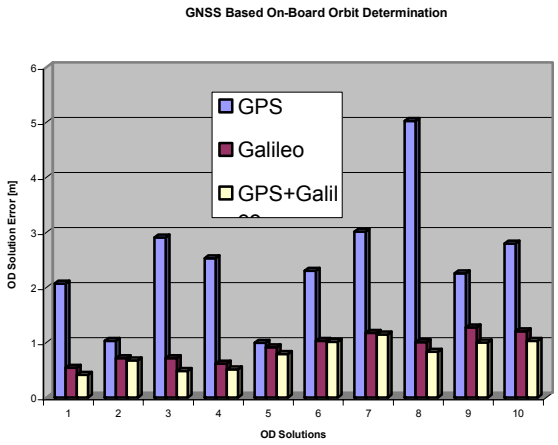

Fig. 6: Results of the Orbit Determination process based on GPS, Galileo and combined signals

Table 8 shows the results obtained from the 10 simulations. GPS with a mean value of around 2.5 m (3D, 1σ) is not compliant with the requirements. Galileo, with a max. of around 1.3 m (3D, 1σ) is compliant with the requirements and could be used within the proposed SAR constellation for real time on-board navigation. In any case, the combination of GPS and Galileo provides a performance max. position error of 1.15 m and mean of 0.8 m (3D, 1σ). This is well within the requirements and assures even a reasonable margin.

3D, 1σ Pos Accuracy [m]	GPS	GAL	GG
Mean	2.494	0.920	0.791
Min	0.999	0.542	0.414
Max	5.026	1.277	1.149

Table 8: Summary of position accuracy achieved for the simulations

In this context it should be clearly high lighted that GPS can perform a real time OD accuracy of 2 m (3D, 1σ) based on the use of observations from C/A and P code. However, the P code option has not been used in this research because the concentration was on civil signals only. In this sense, this investigation reflects a worst case scenario.

Attitude Determination

The AD results obtained within this study are shown in Fig. 7 and Table 9.

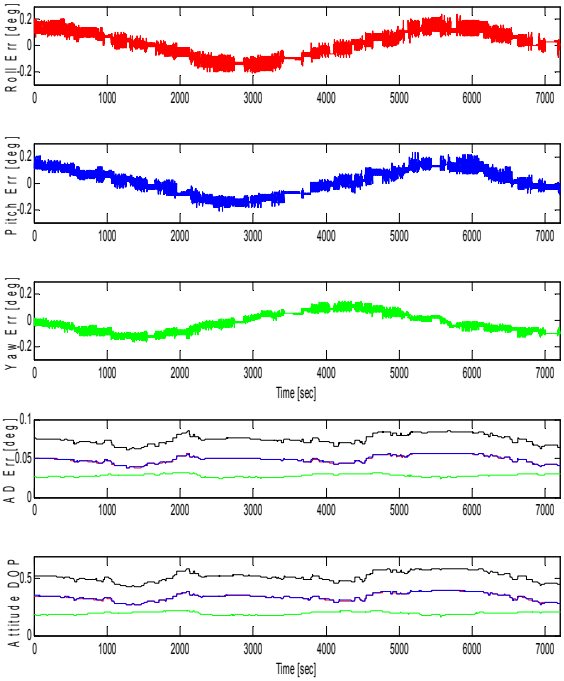

Fig. 7: GNSS based Attitude Determination

	GPS	Galileo	GPS + Galileo
AD Estimation [deg]			
Mean Error Roll	0.01576	0.01704	0.01698
Mean Error Pitch	0.00351	0.01319	0.01015
Mean Error Yaw	-0.03045	-0.01016	-0.01868
1σ Roll	0.10645	0.09802	0.09703
1σ Pitch	0.09865	0.09695	0.09245
1σ Yaw	0.07797	0.07352	0.07069
AD Accuracy [deg]			
Mean Roll	0.07863	0.06297	0.04870
Mean Pitch	0.07996	0.06302	0.04886
Mean Yaw	0.04529	0.03636	0.02797
Mean Attitude 3D	0.12124	0.09631	0.07452
1σ Roll	0.01337	0.00522	0.00479
1σ Pitch	0.01420	0.00510	0.00477
1σ Yaw	0.00432	0.00303	0.00181
1σ Attitude 3D	**0.01810**	**0.00676**	**0.00609**
DOP Mean Values			
Roll	0.54897	0.43963	0.34001
Pitch	0.55827	0.44002	0.34113
Yaw	0.31619	0.25385	0.19531
Attitude 3D	0.84647	0.67242	0.52030

Table 9: Attitude Determination results for the simulated scenarios

Figure 7 and Table 9 shows that the Attitude accuracy requirements for the SAR slave satellites can be met in case of a low multipath environment. The geometry, reflected by the DOP values seems for Galileo to be very good. However, the combined use of GPS and Galileo provides excellent geometry between user and the constellations, so that the DOP values are well below 0.5! Based on the improved signal robustness against multipath in case of Galileo and design considerations for the user satellites, GNSS based AD shows a good potential for space applications.

CONCLUSION

A GNSS based on board navigation concept for a SAR constellation in LEO has been investigated. The investigated concept was not using the most accurate signals available from GPS and from Galileo. The objective was to use services from both systems which are interoperable, compatible and free of charge. For this reason, the civil signals on L1 and L5 in case of GPS and L1 and E5a from Galileo have been used for this investigation. In addition, processing techniques like the carrier smoothing of the Ionospheric free code pseudo ranges, which would improve the accuracy of the measurements have not been applied. This means that the obtained results are not the ultimate regarding achievable accuracy. For this reason, the presented results are reflecting a conservative approach with the clear understanding that the full potential of both systems have not been used to the full extension.

The following statements can be made:

- Real time Orbit Determination with a 3D 1σ position accuracy of better than 1 m can not be achieved by using the investigated GPS observations
- Using Galileo observations will provide real time Orbit Determination 3D 1σ position accuracy of better than 1 m
- The investigated concept shows that real time Orbit Determination 3D 1σ position accuracy of well below 1m (around 80 cm) can be expected in case of a combined use of GPS together with Galileo signals
- Using GPS and Galileo signals together will provide an excellent geometry and related DOP values
- GPS alone could only be used for attitude determination in the investigated low multipath environment in case the requirement is $x < 0.07$ deg 3σ per axis
- Galileo will provide good results for the attitude accuracy, which are well below the SAR requirements (0.016 deg 3σ per axis). Especially the excellent geometry contributes to the performance significantly
- The combined use of carrier phase measurements from GPS and Galileo would provide accuracy in the order of 3D 3σ 0.018 deg for the investigated multipath environment

Further research will be conducted including the relative position vector and variations for improved Signal/Services selection.

The investigated on board navigation concept, based on the next generation of GNSS measurements would be compliant with the identified on board requirements for orbit and attitude of the proposed SAR constellation.

REFERENCES

[1] MASSONNET, D. (1999), 'Capabilities and Limitations of the Interferometric CartWheel'' ,CNES, Toulouse, November 1st, 1999

[2] VACARESSE, ANGELIQUE, BROUSSE, PASCAL (2000): 'Analyse de mission "Roue Interférométrique" associée au satellite japonais ALOS' ,CNES Dèpartement de Mission de Mècanique Spatiale, Division Mathématiques Spatiales, Sema Group , Octobre 2000

[3] RUNGE, H.,R. BAMLER, J. MITTERMAYER, E. F. JOCHIM, D. MASSONNET, E. THOUVENOT (2001): 'The Interferometric CartWheel for Envisat'' ,3rd IAA Symposium on Small Satellites for Earth Observation, April 2-6, 2001 Berlin, Germany

[4] FIEDLER, HAUKE, GERHARD KRIEGER, FRIEDRICH JOCHIM, MICHAEL KIRSCHNER, ALBERTO MOREIRA (2002), 'Analysis of Bistatic Configurations for Spaceborne SAR Interferometry'' , EUSAR 2002, Koeln, 4.-6. Hune 2002, ITG VDE, Proceedings EISAR 2002, VDE Verlag, ISBN: 3-8007-2697-1, pp. 29-32

[5] FIEDLER, HAUKE, GERHARD KRIEGER, FRIEDRICH JOCHIM, MICHAEL KIRSCHNER, ALBERTO MOREIRA (2002), 'Analysis of Satellite Configurations for Spaceborne SAR Interferometry‘' , CNES, Formation Flying, Toulouse, France, 29-31. Oct. 2002, published in: International Symposium Formation Flying Missions & Technologies, Proceedings

[6] FOURCADE, JEAN, LAURENT ARZEL, JACQUES FOLIARD (2002), 'Mission Analysis of Interferometric Wheel Orbit Control‘' ,International Symposium on Formation Flying Mission and Technologies, Toulouse, 29-31 Oct 2002

[7] JOCHIM, E. F., M. KIRSCHNER, H. FIEDLER (HR), G. KRIEGER (HR) (2003): ‘Suitable Orbits for Simultaneous SAR Interferometry’, DLR GSOC TN 2003-04, May 2003

[8] JOCHIM, E. F. (2003): ‘Orbit Aspects of TS-L/CTW Formation Flight’, GSOC TN 2003-06, October 28, 2003

[9] JOCHIM, E. F., KIRSCHNER, M., FIEDLER, H. (2004), ‘Estimation of Fuel Requirement for Bi-Static Orbit Configurations’, DLR-GSOC TN 2004-03, update 2006

[10] D'Amico S., Montenbruck O. (2005), ‘Proximity Operations of Formation Flying Spacecraft using an Eccentricity/Inclination Vector Separation’, AIAA Journal of Guidance, Control and Dynamics, **29**, No.3., May-June 2006, 554-563

[11] MOREIRA, A., G. KRIEGER, J. MITTERMAYER (2002), Satellite Configuration for Interferometric and/or Tomographic Remote Sensing by Means of Synthetic Aperture Radar (SAR), US Patent 6,677,884, July 2002

[12] GALILEO Mission Requirement Document (MRD) (2003), European Commission, Issue 5 – Rev. 1.1, 27. March 2003

[13] GPS-ICD 200

[14] TAPLEY, B. D., SCHUTZ B.E., BORN G.H. (2004): ‘Statistical Orbit Determination’, Elsevier Academic Press

[15] RODRIGUEZ, J., IRSIGLER, M.,HEIN, G. W., PANY, T. (2004), ‘Combined Galileo/GPS Frequency and Signal Performance Analysis’, ION GNSS 2004, USA

[16] SCHLOETZER, S. MARTIN, S. (2005), ‘Performance Study of Multi Carrier Ambiguity Resolution Techniques for Galileo and Modernized GPS’, ION GNSS 2005, USA

[17] HEIN, G. W., RODRIGUEZ, J., (2006), ‘Combining Galileo PRS and M-Code’, Inside GNSS, Januray- February 2006

[18] MCGRAW, G. ‘How can dual frequency code and carrier measurements be optimally combined to enhance position solution accuracy?’ (2006), Inside GNSS, July-August 2006

[19] SIMSKY, A., ‘Three’s the Charm – Triple-Frequency Combinations in Future GNSS’ (2006), Inside GNSS, July-August 2006

[20] Kohlhase, A.O., R. Kroes, S. D'Amico (2006), ‘Interferometric baseline performance estimations for multistatic synthetic aperture radar configurations derived from GRACE GPS observations’, J Geod, DOI 10.1007/s00190-006-0027-y

[21] Enderle W, Walker R A, Feng F, Kellar W, ‘New Dimension for GEO and GTO AOCS Applications Using GPS- And Galileo Measurements’, ION GPS 2002, Portland, Oregon, USA, 24 – 27 September 2002

[22] Zhou, N. Y Feng, W. Enderle, ‘A short-arc batch estimation strategy towards decimetre level GPS-based onboard LEO orbit determination’, ION GPS 2003, Portland, Oregon, USA 10 to 12 September 2003

[23] Cunnigham L.E., On the Computation of the Spherical Harmonic Terms needed during the Numerical Integration of the Orbital Motion of an Artificial Satellite, Celestial Mechanics2, 207-216, 1970

[24] Chiaradia, A. P., Kuga, H. K., ‘The use of the single frequency GPS measurements to determine in real time artificial satellites orbits’, INPE, Technical Note,1999

[25] Markley, F. L., ‘Approximate Cartesian state transition matrix’, The journal of the Astronautical Sciences, Vol. 34, n. 2, p161 – 169, 1986

[26] W. Enderle, A. Dando, ‘The On-Board Orbit and Attitude Determination Concept of the Joint Australian Engineering (Micro) Satellite – JAESat’, 28th ANNUAL AAS GUIDANCE & CONTROL CONFERENCE, Breckenridge, Colorado, USA, February 5 – 9, 2005